

Synthesis of new derivatives of 8-oxoG-Clamp for better understanding the recognition mode and improvement of selective affinity

Li, Zhichun

Graduate School of Pharmaceutical Sciences, Kyushu University

Nakagawa, Osamu

Graduate School of Pharmaceutical Sciences, Kyushu University

Koga, Yohei

Graduate School of Pharmaceutical Sciences, Kyushu University

Taniguchi, Yosuke

Graduate School of Pharmaceutical Sciences, Kyushu University

他

<https://hdl.handle.net/2324/26459>

出版情報 : Bioorganic and Medicinal Chemistry. 18 (11), pp.3992-3998, 2010-06. Elsevier
バージョン :
権利関係 : (C) 2010 Elsevier Ltd.

Synthesis of New Derivatives of 8-oxoG-Clamp for Better Understanding the Recognition Mode and Improvement of Selective Affinity

Zhichun Li, Osamu Nakagawa, Yohei Koga, Yosuke Taniguchi, and Shigeki Sasaki*

Graduate School of Pharmaceutical Sciences, Kyushu University

3-1-1 Maidashi, Higashi-ku, Fukuoka 812-8582, Japan

Tel and Fax: (+) 81-92-642-6615

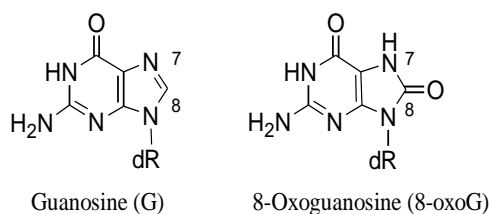
E-mail: sasaki@phar.kyushu-u.ac.jp

Abstract: 8-Oxoguanosine (8-oxoG) is a representative metabolite derived by the oxidation of guanosine (G) and is regarded as a marker of oxidative stress in the cells. We previously reported the 8-oxoG-clamp as the first fluorescent probe for detection of 8-oxoG. In this study, new 8-oxoG-clamp derivatives having a variety of N-functional groups were synthesized and their recognition properties were investigated. The sp³ oxygen atom of the carbamate unit was revealed to play a significant role in the hydrogen bonding interactions, and the pyrene group produced higher stability with 8-oxoG compared with the original 8-oxoG-clamp.

Keywords: 8-oxoguanosine • fluorescent probe • molecular recognition • hydrogen bonding • stacking interaction

Introduction

Reactive oxygen species oxidize nucleic acid components in living organisms to form a variety of oxidized metabolites.¹ Among them 8-oxoguanosine (8-oxoG) is a representative metabolite derived by the oxidation of guanosine (G) and is known to induce G:C to T:A transversion mutations in DNA.² The 8-oxoG level inside and outside cells is regarded as an index of the oxidative damage to cells³ and is believed to have relevance to some diseases⁴ or aging⁵. There are several methods for analysis of 8-oxoG such as HPLC-EC⁶, HPLC/GC-MS,⁷ antibodies in an enzyme-linked immunosorbant assay (ELISA) and immunohistochemical staining of tissues or cells, and so on.^{8,9} Nevertheless, there is a need of more efficient detecting method for 8-oxoG. Our approach has been directed to developing small molecules with high specificity for 8-oxoG, especially those with fluorescence for use in sensors, biological tools and so on. It has been reported from our group that the Cbz-8-oxoG-clamp (**2**), a derivative of G-clamp (**1**), is a selective fluorescent probe for detection of 8-oxoG.¹⁰ Cbz-8-oxoG-clamp (**2**) was also incorporated into the oligodeoxynucleotide (ODN) probe for detection of 8-oxo-dG in DNA. In this study, the new 8-oxoG-clamp derivatives having a variety of *N*-functional groups were synthesized, and their recognition properties were investigated to obtain further insight into the recognition mode and development of the new 8-oxoG-clamp with higher selectivity for 8-oxoG.



Results and Discussion

The formation of five hydrogen bonds has been proved by ¹H-NMR study with the complex of Cbz-8-oxoG-clamp (**2**) and the 8-oxodG derivative (Figure 1B). The substituted group (X) was anticipated to provide both the hydrogen bond and the stacking interaction. However, it was not clear from the ¹H-NMR study whether the carbonyl oxygen of the carbamate group was the acceptor for 7NH and whether the phenyl group of the benzyloxy group provided a stacking interaction. Therefore, in this study, to clarify these questions as well as to achieve higher affinity for 8-oxoG, new 8-oxoG-clamp derivatives having a variety of *N*-substituted groups (Figure 1A) have been synthesized and their recognition properties have been evaluated.

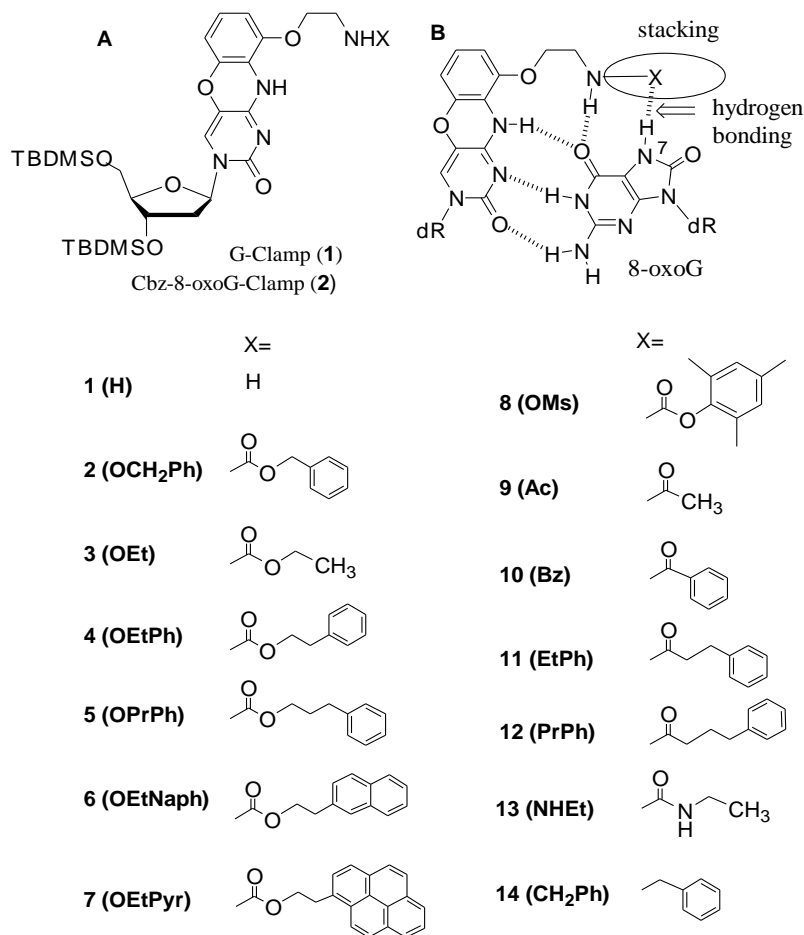


Figure 1. The structure of the 8-oxoG-clamp synthesized in this study (A), and the *N*-X group expected for stacking and hydrogen bonding (B).

The carbamate derivatives (**3-8**) were prepared by a coupling reaction of **1** with the alkoxy carbonylimidazole which was obtained with the corresponding alcohol and carbonyldiimidazole. The ureido group was similarly introduced using ethylamine (**13**). The acyl derivatives (**9-12**) were obtained using the corresponding acyl chlorides. The benzyl derivative (**14**) was synthesized by the reaction of **1** with benzaldehyde in the presence of Mg_2SO_4 in refluxing CH_2Cl_2 , followed by reduction with NaBH_3CN in MeOH.

The recognition property of the 8-oxoG-clamp derivative was evaluated by measuring fluorescence quenching phenomena by the addition of the nucleoside derivative. The 3'-*O*-, 5'-*O*-di-TBDMS (tertbutyldimethylsilyl) protected nucleoside was added to a solution of the 8-oxoG-clamp derivative in CHCl_3 buffered with 10 mM ETA and 2.7 mM AcOH at 25 °C. The fluorescence spectra were recorded with the

excitation wavelength at 365 nm, and the change with the addition of the nucleoside derivative was followed. Figure 2 illustrates an example with the 8-oxoG-clamp (**7**, OEtPyr), demonstrating the selective quenching by the 8-oxodG derivative and almost negligible quenching by other nucleoside derivatives.

The titration data thus obtained were analyzed by the curve-fitting method to give the equilibrium binding constants, which are summarized in Figure 3 (data are listed in Table 1). As the derivative of dA, dC or dT did not quench efficiently the fluorescence of the oxoG-clamp derivative as shown in Figure 2, nor did dG to the 8-oxoGclamp derivatives (**2-12** and **14**), their data are not shown. The G-clamp (**1**) with the amino terminal showed almost the same binding constants for 8-oxodG and dG. In contrast, the 8-oxoG-clamp (**2**) was quenched selectively by 8-oxodG as previously reported. It was anticipated that the benzyloxy group contributed to the complex formation as a stacking unit. However, the derivative **3** (OEt) without the benzene group exhibited a slightly higher binding affinity to 8-oxodG.

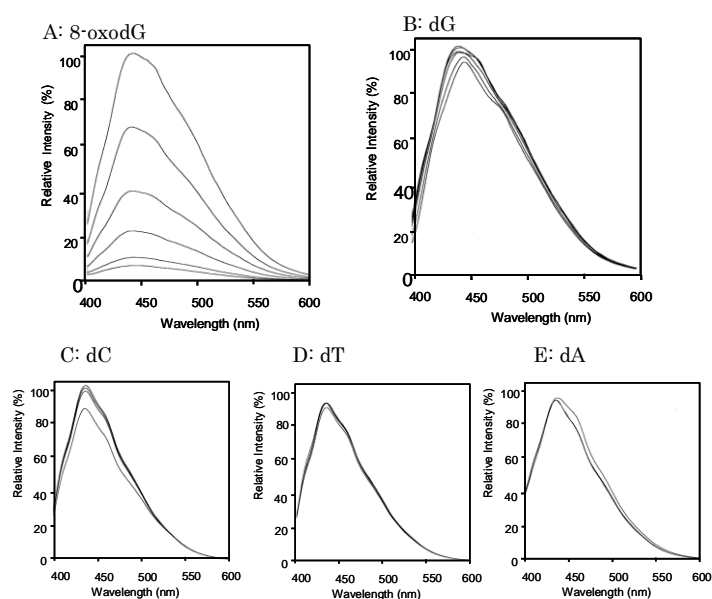


Figure 2. Fluorescence quenching of the 8-oxoG-clamp (**7**, OEtPyr). The 3'-O-, 5'-O-di TBS protected 2'-deoxynucleoside (0-10 μ M final concentration) was added to a solution of **7** (1 μ M) in CHCl_3 containing 10 mM ETA and 2.7 mM AcOH at 25 $^\circ\text{C}$. Fluorescence spectra were recorded with excitation at 365 nm.

Considering that a stacking interaction requires a well-defined contact between two aromatic groups,¹¹ we further investigated the effect of the size and the length of the aromatic group (**4-7**) with varying the linker from ethyl to propyl and the aromatic group from benzene to pyrene. Interestingly, the binding affinity increased with **4** (OEtPh) but decreased with **5** (OPrPh). As the ethyl group attached to the benzene ring seemed to be better than the methyl group of **2** or the propyl group of **5**, the naphthalene (**6**) and the pyrene unit (**7**) were introduced as a larger aromatic ring through the ethyl linker. Eventually, it was found that oxoG-clamp (**7**) with the ethyl-linked pyrene produced a great improvement in binding affinity.

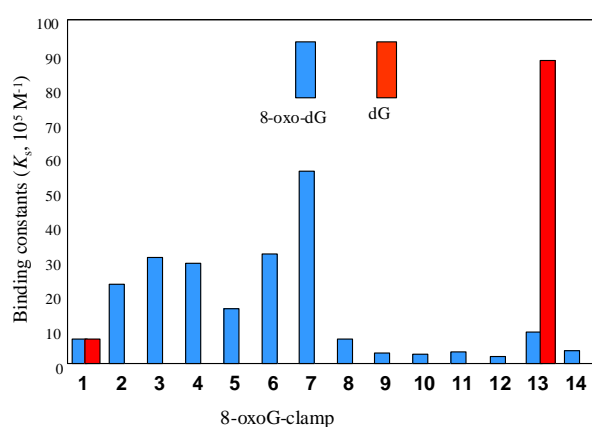


Figure 3. Equilibrium binding constants obtained by fluorescence quenching experiments in buffered CHCl₃ (K_s , 10⁵ M⁻¹). The bars represent the binding constants with 8-oxo-dG (blue bars) and those with dG (red bars). Titration experiments were performed by the method described in the footnote to Figure 2, and analyzed by the curve-fitting method. Data of **1**, **2**, **9** and **10** were already reported in the reference 10c.

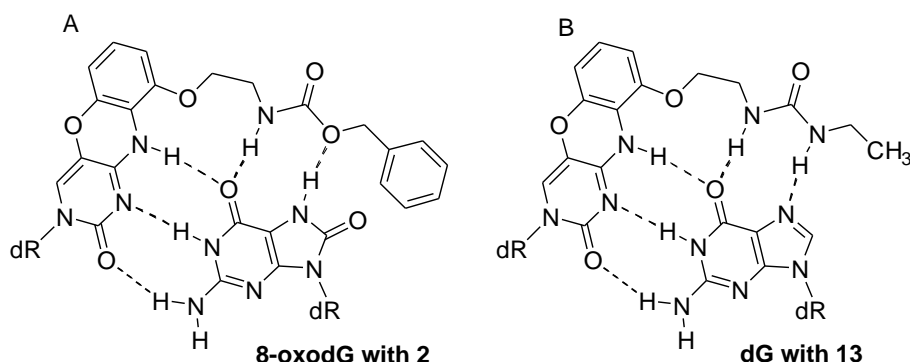


Figure 4. Possible complex structures formed with 8-oxodG (A) and dG (B). (A) The revised mode of the complex with 8-oxodG for inclusion of the hydrogen bond

between the sp^3 oxygen of the carbamate and 7-NH of 8-oxodG. (B) The NH of the ureido group may form the hydrogen bond with 7N of dG.

Notably, the acyl derivatives (**9-12**) showed lower affinity than the corresponding carbamate derivatives, leading to an assumption that the sp^3 oxygen rather than the carbonyl oxygen of the carbamate group is included in the hydrogen bond formation with 8-oxo-dG. The low affinity of the carbamate-type **8** may be rationalized in terms of the steric hindrance of the 2,6-dimethyl groups of the benzene for the interaction to the sp^3 oxygen. The facts that **10** and its reductive form **14** with the *N*-benzyl group showed almost the same binding constants are also indicative of less importance of the carbonyl oxygen of the carbamate group. On the other hand, the ureido derivative **13** with the NH group as a H-donor instead of the sp^3 oxygen for the H-acceptor in hydrogen bond formation expressed a 10 times higher affinity for dG than for 8-oxo-dG. It has been concluded from these results that the sp^3 oxygen atom of the carbamate group is involved in the hydrogen bond formation with 8-oxodG and is responsible for the selectivity for the 8-oxoG-clamp, as illustrated in Figure 4.

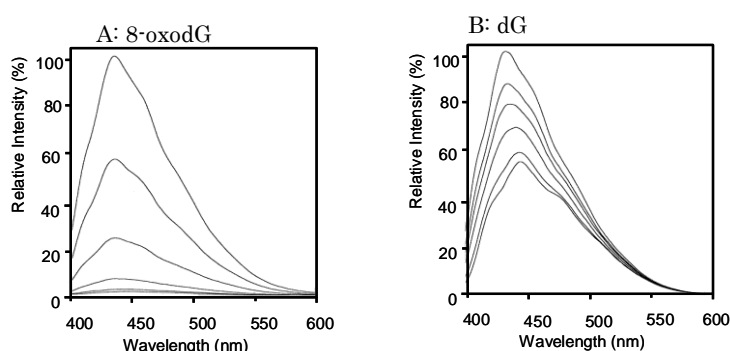


Figure 5. Fluorescence quenching experiments in the non-buffered $CHCl_3$ solution. The experiments were performed under the same conditions described in the footnote to Figure 2, except that TEA and AcOH were not included in $CHCl_3$ solution.

To gain further insight into the effects of the *N*-substituted group on the binding constants, binding experiments were performed in the non-buffered $CHCl_3$ solution. When the components of 10 mM TEA and 2.7 mM AcOH are dissolved in water, the solution is buffered at pH 7.0. In the meantime, these components also make the organic solutions polar to some extent, namely the non-buffered $CHCl_3$ solutions provide a less polar medium compared to the buffered ones. In non-buffered $CHCl_3$,

dG also induces fluorescence quenching, and the equilibrium binding constants can be obtained accurately (Figure 5, A vs B). The fluorescence quenching is thought to occur by a photo-induced electron transfer mechanism, which depends strongly on the distance between the fluorophore and the quencher.¹² Because the hydrogen bond becomes stronger in non-buffered CHCl_3 than that in buffered CHCl_3 , 8-oxoG-clamp and dG become closer enough for induction of fluorescence quenching.

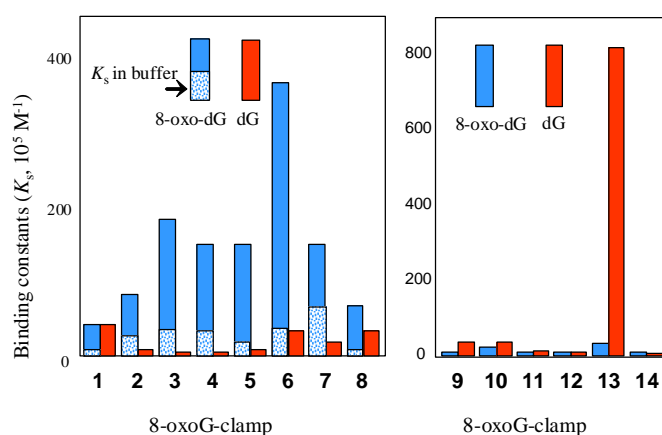


Figure 6. Equilibrium binding constants obtained by fluorescence quenching experiments in non-buffered CHCl_3 ($K_s, 10^5 \text{ M}^{-1}$). Titration experiments were performed by the method described in the footnote to Figure 2, except that TEA and AcOH were not added to the solution.

The equilibrium binding constants obtained in non-buffered CHCl_3 are compared in Figure 6 (data are listed in Table 2). The K_s values obtained in the buffered solution (Figure 3) overlapped the bar graphs of the carbamate-type oxoG-clamp (2-8). Interestingly, the effects of the carbamate structure on the binding constants were different from those observed in the buffered CHCl_3 solution. The binding constants of 3, 4, 5 and 7 were almost the same, but the highest was obtained with 6, suggesting possible involvement of a stacking interaction between the naphthalene and the 8-oxoguanosine part. Possible complex structures were simulated by MO calculation (MOPAC, PM6) and some examples are summarized in Figure 7. Figure 7B illustrates a face-to-face orientation between the pyrene group and 8-oxoG and Figure 7C shows close contacts suitable for the formation of the hydrogen bonds in the complex between 7 (OEtPyr) and the 8-oxoG. This molecular modeling also suggests that the ethyl linker between the sp^3 oxygen of the carbamate and the pyrene ring is suitable for orienting the aromatic ring for such a face-to-face contact. The complex structures were also calculated with the TBDMS-protected sugar structure, and have suggested that, as the

pyrene ring has a larger aromatic plane than naphthalene, it causes steric repulsion toward the sugar parts within a compact complex (Figures 7D vs 7E). The binding affinity of **6** decreased in the buffered CHCl_3 solution ($K_{\text{buffered}} / K_{\text{non-buffer}} = 0.1$) to a larger extent than that of **7** ($K_{\text{buffered}} / K_{\text{non-buffer}} = 0.43$). It is likely that stacking interaction with the naphthalene ring becomes weaker and that with the pyrene group is kept in a polar medium.¹³

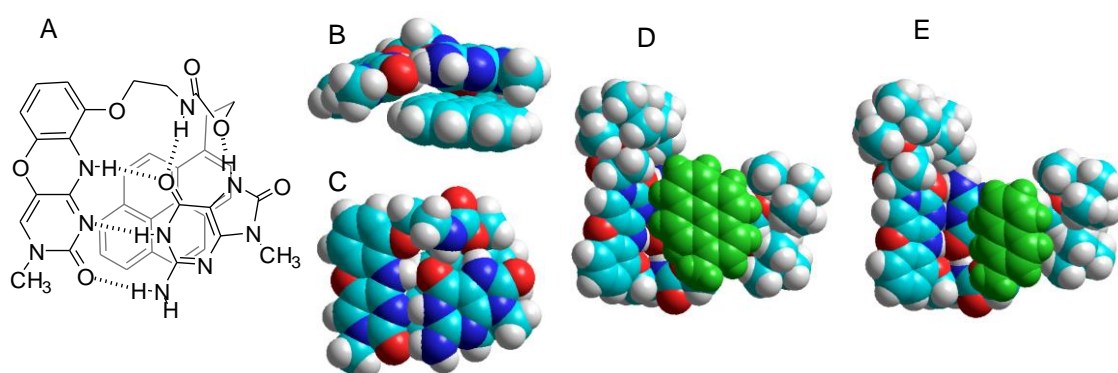


Figure 7. A simulated complex structure between **7** (OEtPyr) and the 8-oxoG. The 2'-deoxyribose part was replaced by the methyl group for simplification in MO calculation in A-C, and the protected derivatives were used in simulation of D and E (MOPAC2009, PM6). (A) The dashed lines represent a distance less than 2.5-2.6 Å. Gray lines show the structure at the back side. (B) The side view of the complex illustrates a face-to-face orientation between the pyrene group and 8-oxoG. (C) The top view of the complex shows the close contact for the formation of hydrogen bonds. (D) The view from the side of the pyrene ring shown in green. (E) The view from the side of the naphthalene ring shown in green of the complex between **6** (OEtNaph) and the 8-oxoG.

Conclusion

This study was aimed at clarifying whether the carbonyl oxygen or the sp^3 oxygen of the carbamate group is involved in the complex formation with 8-oxoguanosine. Quantitative evaluation of the equilibrium binding constants of the new 8-oxoG-clamp derivatives with a variety of *N*-functional groups has clearly indicated that the sp^3

oxygen of the carbamate group is responsible for selective complexation with 8-oxoguanosine. Another purpose of this study was to determine the appropriate structure of the *N*-functional group, especially in terms of the stacking interaction, for obtaining better recognition molecules for 8-oxoguanosine. As a result, the new oxoG-clamp derivative (**7**) with the 2-pyren-1-yl-ethoxycarbonyl unit has been determined to be a better recognition molecule for 8-oxo-dG. These new oxoG-clamp derivatives and the clarified binding mode will be useful for further design of the molecules that may be used for recognition of 8-oxoG in nucleic acids as well as for the purpose of 8-oxoG detection in water.

Experimental Section

OEt-8-oxoG-clamp (3). Under Ar atmosphere, *N,N'*-carbodiimidazole was added into a solution of ethanol (250 μ L) in dry CH_2Cl_2 (10 mL), and the mixture was stirred for 2.5 h at room temperature. Evaporation of the solvents gave a crude product, which was crystallized from n-hexane to give a white powder (imidazole:1H-imidazole-1-carboxylic acid ethyl ester = 12 : 1 by NMR). The above powder (36 mg, 0.036 mmol) was added into a solution of **1** (20 mg, 0.033 mmol) in dry CH_3CN (0.5 ml), and the mixture was stirred for 24 h. The reaction mixture was quenched with aqueous NaHCO_3 (10 mL) and extracted with CHCl_3 (20 mL). The organic layers were evaporated to give a crude oil, which was chromatographed on a silica gel column (AcOEt:n-hexane = 1:1 to give **3** (13 mg, 57%). $^1\text{H-NMR}$ (400MHz, CDCl_3) δ : 7.61 (1H, s), 7.77 (1H, t, $J = 9$ Hz), 6.45 (1H, d, $J = 8$ Hz), 6.35 (1H, d, $J = 8$ Hz), 6.25 (1H, t, $J = 6$ Hz), 5.79 (1H, br), 4.37 (1H, m), 4.11 (2H, m), 4.03 (2H, t, $J = 5$ Hz), 3.90 (3H, m), 3.75 (1H, d), 3.55 (2H, q), 2.37 (1H, m), 2.09 (1H, m), 1.24 (3H, m), 0.94 (9H, s), 0.86 (9H, s), 0.14 (3H, s), 0.12 (3H, s), 0.04 (6H, s). $^{13}\text{C NMR}$ (125 MHz, CDCl_3) δ : 156.9, 146.7, 143.2, 127.3, 124.1, 122.6, 108.4, 107.3, 87.6, 86.0, 70.8, 68.6, 62.3, 61.0, 41.9, 40.4, 26.0, 25.7, 18.5, 18.0, 14.6, -4.6, -4.9, -5.5, -5.5. IR ν_{max} (film): 2929, 1695, 1473, 1099 cm^{-1} . High-resolution MS (ESI): Calcd for $\text{C}_{32}\text{H}_{53}\text{N}_4\text{O}_8\text{Si}_2$ ($\text{M}+\text{H}$) $^+$: 677.3397. Found: 677.3410.

OEtPh-8-oxoG-clamp (4). Under Ar atmosphere, *N,N'*-carbodiimidazole was added into a solution of 2-phenylethanol (500 mg) in dry CH_2Cl_2 (10 mL), and the mixture was stirred for 2.5 h at room temperature. Evaporation of the solvents gave a crude product, which was crystallized from n-hexane to give a white powder

(imidazole:1H-imidazole-1-carboxylic acid 2-phenylethyl ester = 4 : 1 by NMR). The above power (20 mg, 0.036 mmol) was added into a solution of **1** (20 mg, 0.033 mmol) in dry CH₃CN (0.5 ml), and the mixture was stirred for 24 h. The reaction mixture was quenched with aqueous NaHCO₃ (10 mL) and extracted with CHCl₃ (10 mL). The organic layers were evaporated to give a crude oil, which was chromatographed on a silica gel column (AcOEt:n-hexane = 1:1 to give **4** (8 mg, 34%). ¹H-NMR (400MHz, CDCl₃) δ: 7.65 (1H, s), 7.25 (3H, m), 7.18 (2H, m), 6.78 (1H, t, *J* = 8 Hz), 6.44 (1H, d, *J* = 9 Hz), 6.35 (1H, d, *J* = 8 Hz), 6.26 (1H, t, *J* = 6 Hz), 5.93 (1H, br), 4.37 (1H, m), 4.26 (2H, t, *J* = 7 Hz), 4.02 (2H, m), 3.91 (3H, m), 3.75 (1H, m), 3.55 (2H, m), 2.91 (2H, t, *J* = 7 Hz), 2.35 (1H, m), 2.08 (1H, m), 0.94 (9H, s), 0.86 (9H, s), 0.14 (3H, s), 0.12 (3H, s), 0.04 (6H, s). ¹³C NMR (125 MHz, CDCl₃) δ: 156.8, 143.2, 129.0, 128.4, 126.4, 108.3, 107.3, 87.8, 9.1, 70.8, 68.5, 65.4, 62.3, 42.0, 40.4, 35.6, 26.0, 25.7, 18.5, 18.0, -4.6, -4.9, -5.5, -5.5. IR ν_{max} (film): 2929, 1701, 1473, 1276 cm⁻¹. High-resolution MS (ESI): Calad for C₃₈H₅₇N₄O₈Si₂ (M+H)⁺: 753.3710. Found 753.3719.

OprPh-8-oxoG-clamp (5). Under Ar atmosphere, *N,N'*-carbodiimidazole was added into a solution of 3-phenyl-1-propanol (500 mg) in dry CH₂Cl₂ (10 mL), and the mixture was stirred for 2.5 h at room temperature. Evaporation of the solvents gave a crude product, which was crystallized from n-Hexane to give a white powder (imidazole:1H-imidazole-1-carboxylic acid 3-phenyl propyl ester = 3 :1 by NMR). The above power (14 mg, 0.027 mmol) was added into a solution of **1** (15 mg, 0.025 mmol) in dry CH₃CN (0.5 ml), and the mixture was stirred for 24 h. The reaction mixture was quenched with aqueous NaHCO₃ (10 mL) and extracted with CHCl₃ (10 mL). The organic layers were evaporated to give a crude oil, which was chromatographed on a silica gel column (AcOEt:n-hexane = 1:1 to give **5** (12 mg, 63%). ¹H-NMR (400MHz, CDCl₃) δ: 7.67 (1H, s), 7.25 (2H, m), 7.15 (3H, m), 6.80 (1H, t, *J* = 9 Hz), 6.47 (1H, d, *J* = 9 Hz), 6.37 (1H, d, *J* = 8 Hz), 6.25 (1H, t, *J* = 6 Hz), 5.75 (1H, br), 4.38 (1H, m), 4.10 (2H, m), 4.05 (2H, m), 3.92 (2H, m), 3.77 (1H, dd), 3.57 (2H, m), 2.67 (2H, m), 2.37 (1H, m), 2.07 (1H, m), 1.94 (2H, m), 0.94 (9H, s), 0.86 (9H, s), 0.14 (3H, s), 0.12 (3H, s), 0.05 (6H, s). ¹³C NMR (125 MHz, CDCl₃) δ: 157.95, 146.8, 143.2, 128.4, 128.3, 127.1, 125.8, 124.6, 108.4, 107.3, 87.8, 86.1, 70.8, 68.5, 64.4, 62.3, 42.0, 40.4, 32.1, 30.6, 26.0, 25.7, 18.5, 18.0, -4.6, -4.9, -5.5, -5.5. IR ν_{max} (film): 3082, 2955, 1696, 1474 cm⁻¹. High-resolution MS (ESI): Calad for C₃₉H₅₉N₄O₈Si₂ (M+H)⁺: 767.3866. Found 767.3913.

OEtNap-8-oxoG-clamp (6). Under Ar atmosphere, *N,N'*-carbodiimidazole was added into a solution of 1-naphthaleneethanol (700 mg) in dry CH₂Cl₂ (10 mL), and the mixture was stirred for 1.5 h at room temperature. Evaporation of the solvents gave a

crude product, which was crystallized from ether to give a white powder (imidazole:1H-imidazole-1-carboxylic acid 2-(2-naphthyl) ethyl ester = 3:1 by NMR). The above power (13 mg, 0.027 mmol) was added into a solution of **1** (15 mg, 0.025 mmol) in dry CH₃CN (1 ml), and the mixture was stirred for 24 h. The reaction mixture was quenched with aqueous NaHCO₃ (10 mL) and extracted with CHCl₃ (15 mL). The organic layers were evaporated to give a crude oil, which was chromatographed on a silica gel column (CHCl₃/MeOH = 100 :1 to give **6** (15 mg, 74%). ¹H-NMR (400MHz, CDCl₃) δ: 8.07 (1H, m), 7.80 (1H, d, *J* = 8 Hz), 7.69 (1H, dd), 7.60 (1H, s), 7.45 (2H, m), 7.36 (2H, m), 6.76 (1H, t, *J* = 8 Hz), 6.43 (1H, d, *J* = 8 Hz), 6.36 (1H, d, *J* = 8 Hz), 6.28 (1H, t), 5.80 (1H, br), 4.39 (4H, m), 4.01 (1H, m), 3.91 (2H, m), 3.76 (1H, m), 3.54 (1H, m), 3.38 (3H, m), 2.37 (1H, m), 2.09 (1H, m), 0.94 (9H, s), 0.86 (9H, s), 0.14 (3H, s), 0.12 (3H, s), 0.05 (6H, s). ¹³C NMR (125 MHz, CDCl₃) δ: 156.8, 153.1, 152.1, 146.7, 143.2, 133.8, 132.1, 128.7, 127.3, 127.0, 126.1, 125.5, 125.5, 123.7, 108.4, 107.3, 87.6, 86.0, 70.8, 68.5, 65.0, 62.3, 41.9, 40.4, 32.7, 26.1, 25.7, 18.5, 18.0, -4.6, -4.9, -5.5, -5.5. IR ν_{max} (film): 2857, 1693, 1474, 1255. High-resolution MS (ESI): Calcd for C₄₂H₅₉N₄O₈Si₂ (M+H)⁺: 803.3866. Found 803.3862.

1-Pyrenyl-2-ethanol. Under Ar atmosphere, a solution of 1-pyrenyl acetic acid (200 mg, 0.77 mmol) in 3.5 mL dry THF was added into a suspension of LiAlH₄ (117 mg, 3.07 mmol) in dry THF (2.5 mL), and the mixture was stirred for 2h at room temperature. The reaction mixture was quenched by a sequential addition of methanol (2.5 mL) and 10% aqueous H₂SO₄, and extracted with ether. The organic layers were dried over Na₂SO₄, evaporated to give a crude oil, which was chromatographed on a silica gel column (CHCl₃) to give 1-pyrenyl-2-ethanol (160 mg, 84%). ¹H-NMR (400MHz, CDCl₃) δ: 8.35 (1H, m), 8.16 (4H, m), 7.96 (4H, m), 3.98 (2H, t, *J* = 7 Hz), 3.58 (2H, t, *J* = 7 Hz). IR ν_{max} (film): 3293, 2324, 1044, 841. ESI-MS(m/z): 247.0883(M+H)⁺.

OEtPyr-8-oxoG-clamp (7). Under Ar atmosphere, *N,N'*-carbodiimidazole was added into a solution of 1-pyrenylethanol (160 mg) in dry CH₂Cl₂ (2.5 mL), and the mixture was stirred for 2.5 h at room temperature. Evaporation of the solvents gave a crude product, which was crystallized from ether to give a white powder (imidazole:1H-imidazole-1-carboxylic acid 1-pyrenyl-2-ethanol ester = 3:1 by NMR). The above power (18 mg, 0.028 mmol) was added into a solution of **1** (15 mg, 0.025 mmol) in dry CH₃CN (1 ml), and the mixture was stirred for 24 h. The reaction mixture was quenched with aqueous NaHCO₃ (10 mL) and extracted with CHCl₃ (15 mL). The organic layers were evaporated to give a crude oil, which was chromatographed on a silica gel column (AcOEt:n-hexane = 1:1 to give **7** (14 mg, 65%). ¹H-NMR (400MHz,

CDCl₃) δ : 8.34 (1H, d, J = 9 Hz), 8.08 (4H, m), 7.93 (4H, m), 7.70 (1H, s), 6.84 (1H, t, J = 9 Hz), 6.67 (1H, br), 6.42 (1H, d, J = 9 Hz), 6.32 (1H, d, J = 8 Hz), 6.21 (1H, t, J = 6 Hz), 4.49 (2H, m), 4.36 (1H, m), 3.98 (2H, m), 3.94 (2H, m), 3.76 (1H, m), 3.66 (2H, m), 3.61 (2H, m), 2.36 (1H, m), 2.05 (1H, m), 0.94 (9H, s), 0.87 (9H, s), 0.15 (3H, s), 0.13 (3H, s), 0.05 (6H, s). ¹³C NMR (125 MHz, CDCl₃) δ : 172.7, 153.1, 146.3, 143.0, 140.7, 128.3, 127.4, 126.1, 123.7, 122.8, 115.7, 108.3, 106.8, 87.6, 86.0, 70.8, 68.0, 62.3, 42.0, 38.8, 38.2, 31.7, 26.0, 25.7, 18.5, 17.9, -4.6, -4.9, -5.5, -5.5. IR ν_{\max} (film): 2951, 2323, 1696, 1473 cm⁻¹. High-resolution MS (ESI): Calcd for C₄₈H₆₁N₄O₈Si₂ (M+H)⁺: 877.4023. Found 877.4062.

OMs-8-oxoG-clamp (8). Under Ar atmosphere, *N,N'*-carbodiimidazole was added into a solution of 2,4,6-trimethyl phenol (270 mg) in dry CH₂Cl₂ (5 mL), and the mixture was stirred for 2.5 h at room temperature. Evaporation of the solvents gave a crude product, which was crystallized from n-Hexane to give a white powder (imidazole:1H-imidazole-1-carboxylic acid 2,4,6-trimethyl phenyl ester = 2:1 by NMR). The above powder (12 mg, 0.043 mmol) was added into a solution of **1** (16 mg, 0.026 mmol) in dry CH₃CN (0.5 ml), and the mixture was stirred for 24 h. The reaction mixture was quenched with aqueous NaHCO₃ (10 mL) and extracted with CHCl₃ (10 mL). The organic layers were evaporated to give a crude oil, which was chromatographed on a silica gel column (AcOEt:n-hexane = 1:1) to give **8** (2 mg, 10%). ¹H-NMR (400MHz, CDCl₃) δ : 7.64 (1H, s), 6.81 (2H, m), 6.78 (1H, t), 6.48 (1H, d, J = 8 Hz), 6.39 (1H, d), 6.27 (1H, t), 4.38 (1H, m), 4.10 (2H, m), 3.89 (2H, m), 3.76 (2H, m), 3.58 (2H, m), 2.38 (1H, m), 2.23 (3H, s), 2.11 (7H, m), 0.95 (9H, s), 0.86 (9H, s), 0.15 (3H, s), 0.13 (3H, s), 0.05 (6H, s). IR ν_{\max} (film): 2952, 2322, 1712, 1474 cm⁻¹. High-resolution MS(ESI): calcd for C₃₉H₅₉N₄O₈Si₂ (M+H)⁺: 767.3866. Found 767.3841.

Et-Ph-8-oxoG-clamp (11). Under Ar atmosphere, 3-phenylpropionyl chloride (7 μ l, 0.05 mmol) and Et₃N (12 μ l, 0.08 mmol) were added to a solution of compound **1** (25 mg, 0.04 mmol) in anhydrous THF (0.5 ml) at 0°C and the mixture was stirred at room temperature for 1 h. The reaction mixture was quenched by addition of saturated NaHCO₃ solution. The mixture was extracted with CHCl₃. The organic phase was washed with water and brine and dried over Na₂SO₄ and concentrated under reduced pressure. The residue was purified by silica gel column chromatography (CHCl₃/MeOH = 95/5) afforded compound **11** (19 mg, 62%) as a yellow crystals. ¹H-NMR (400MHz, CDCl₃) δ : 7.63 (1H, s), 7.15 (4H, m), 7.06 (1H, m), 6.77 (1H, t, J = 8 Hz), 6.49 (1H, br), 6.37 (2H, m), 6.23 (1H, t, J = 6 Hz), 4.37 (1H, m), 3.94 (2H, m), 3.89 (2H, m), 3.75 (1H, d, J = 11 Hz), 3.58 (2H, m), 2.93 (2H, t, J = 8 Hz), 2.50 (2H, t, J = 8 Hz), 2.34 (1H, m),

2.05 (1H, m), 0.90 (9H, s), 0.86 (9H, s), 0.13 (3H, s), 0.10 (3H, s), 0.04 (6H, s). IR ν_{\max} (film): 2929, 1671, 1558, 1473. ESI-MS (m/z): 737.5 (M+H)⁺.

PrPh-8-oxoG-clamp (12) Under Ar atmosphere DCC (9 mg, 0.044 mmol), DMAP (2 mg, 0.019 mmol) and **1** (19 mg, 0.032 mmol) were added to a solution of 4-phenyl-n-butyric acid (6 mg, 0.038 mmol) in anhydrous dichloromethane (2 ml) at room temperature and the mixture was stirred for 1 h. Evaporation of the solvents gave a crude product, which was purified by silica gel column chromatography (CHCl₃/MeOH = 95/5) to give compound **12** (22 mg, 82%) as a yellow crystals. ¹H-NMR (400MHz, CDCl₃) δ : 7.62 (1H, s), 7.21 (2H, m), 7.12 (3H, m), 6.77 (1H, t, J = 8 Hz), 6.57 (1H, br), 6.44 (1H, d, J = 8 Hz), 6.34 (1H, d, J = 8 Hz), 6.23 (1H, t, J = 6 Hz), 4.37 (1H, m), 4.03 (2H, m), 3.92 (1H, d, J = 11 Hz), 3.88 (1H, m), 3.76 (1H, d, J = 11 Hz), 3.62 (2H, m), 2.60 (2H, t, J = 8 Hz), 2.33 (1H, m), 2.21 (2H, t, J = 8 Hz), 2.03 (1H, m), 1.94 (2H, m), 0.94 (9H, s), 0.80 (9H, s), 0.14 (3H, s), 0.12 (3H, s), 0.05 (6H, s). ¹³C NMR (125 MHz, CDCl₃) δ : 173.3, 153.1, 146.4, 143.1, 141.6, 128.4, 128.3, 127.3, 125.9, 123.9, 122.8, 115.6, 108.4, 106.8, 87.6, 86.0, 70.8, 68.1, 62.3, 45.0, 38.8, 35.9, 35.2, 27.1, 26.1, 25.7, 18.5, 18.0, -4.6, -4.9, -5.5, -5.5. IR ν_{\max} (film): 2952, 1671, 1558, 1473, 1256. ESI-MS (m/z): 751.5 (M+H)⁺.

NHEt-8-oxoG-clamp (13). Under Ar atmosphere, *N,N'*-carbodiimidazole was added into a solution of ethylamine (70% in water) (500 μ L) in dry CH₂Cl₂ (10 mL), and the mixture was stirred for 2.5 h at room temperature. Evaporation of the solvents gave a crude product, which was crystallized from n-Hexane to give a white powder (imidazole:1H-imidazole-1-carboxylic acid *N*-ethyl ester = 3:1 by NMR). The above powder (16 mg, 0.036 mmol) was added into a solution of **1** (15 mg, 0.025 mmol) in dry CH₃CN (0.5 ml), and the mixture was stirred for 24 h. The reaction mixture was quenched with aqueous NaHCO₃ (10 mL) and extracted with CHCl₃ (10 mL). The organic layers were evaporated to give a crude oil, which was chromatographed on a silica gel column (CHCl₃/MeOH = 50:1) to give **13** (11 mg, 65%). ¹H-NMR (400MHz, CDCl₃) δ : 7.61 (1H, s), 6.7 (1H, t, J = 8 Hz), 6.46 (1H, d, J = 8 Hz), 6.33 (1H, d, J = 8 Hz), 6.21 (1H, t, J = 6 Hz), 5.72 (1H, br), 4.91 (1H, br), 4.36 (1H, m), 4.04 (2H, m), 3.91 (1H, m), 3.87 (1H, m), 3.75 (1H, m), 3.57 (1H, m), 3.20 (2H, m), 2.33 (1H, m), 2.05 (1H, m), 1.11 (3H, t, J = 7 Hz), 0.94 (9H, s), 0.86 (9H, s), 0.14 (3H, s), 0.12 (3H, s), 0.05 (6H, s). ¹³C NMR (125 MHz, CDCl₃) δ : 158.8, 153.2, 152.9, 146.8, 143.0, 127.6, 122.7, 115.4, 108.4, 108.2, 107.4, 87.7, 86.0, 70.8, 69.3, 62.3, 41.9, 39.4, 35.4, 25.7, 25.0, 18.5, 17.9, 15.5, -4.6, -4.9, -5.5, -5.5. IR ν_{\max} (film): 3318, 1673, 1350, 1169 cm⁻¹. High-resolution MS (ESI): calad for C₃₂H₅₄N₅O₇Si₂ (M+H)⁺: 676.3556. Found 676.3602.

CH₂Ph-8-oxoG-clamp (14) Under Ar atmosphere benzaldehyde (6 μ l, 0.06 mmol) and MgSO₄ (30 mg) were added to a solution of compound **1** (30 mg, 0.05 mmol) in anhydrous dichloromethane (2 ml) at room temperature and the mixture was refluxed for 15 h. The reaction mixture was filtered to remove the magnesium sulfate. and the solvent was concentrated under reduced pressure gave a crude product. Without farther purified, To a stirred solution of the above crude product (37 mg) in methanol (2 ml) was added 10 mg (0.16 mmol) of sodium cyanoborohydride. The reaction mixture was stirred at room temperature for 1 h. The reaction was quenched by addition of water. The mixture was extracted with CHCl₃. The organic phase was dried over Na₂SO₄ and concentrated under reduced pressure. The residue was purified by silica gel column chromatography (CHCl₃/MeOH = 95/5) afforded compound **14** (21 mg, 57%) as a yellow crystals. ¹H-NMR (400MHz, CDCl₃) δ : 7.60 (1H, s), 7.33 (4H, m), 7.23 (1H, m), 6.73 (1H, t, *J* = 8 Hz), 6.46 (1H, d, *J* = 8 Hz), 6.35 (1H, d, *J* = 8 Hz), 6.23 (1H, t, *J* = 6 Hz), 4.37 (1H, m), 4.08 (2H, m), 3.92 (3H, m), 3.87 (1H, m), 3.75 (1H, d, *J* = 11 Hz), 3.01 (2H, m), 2.36 (1H, m), 2.05 (1H, m), 0.94 (9H, s), 0.86 (9H, s), 0.14 (3H, s), 0.12 (3H, s), 0.05 (6H, s). ¹³C NMR (125 MHz, CDCl₃) δ : 154.1, 153.5, 146.2, 143.0, 128.5, 127.5, 127.4, 123.2, 122.6, 116.6, 108.6, 108.0, 87.5, 85.9, 70.7, 68.8, 62.3, 53.3, 47.5, 42.0, 26.0, 25.7, 18.5, 18.0, -4.6, -4.9, -5.5, -5.3. IR ν_{\max} (film): 2928, 1671, 1558, 1473. ESI-MS(*m/z*): 695.6 (M+H)⁺.

Table 1. Equilibrium binding constants of 8-OxoG-clmap derivatives with dG and 8-oxo-dG derivatives obtained by fluorescence quenching experiments in buffered CHCl₃ (*K_s*, 10⁵ M⁻¹)^a.

| Compound | 1 | 2 | 3 | 4 | 5 | 6 | 7 |
|----------|----------|----------|-----------|-----------|-----------|-----------|-----------|
| oxodG | 7.3 | 23 | 31 | 29 | 16 | 32 | 56 |
| dG | 7.1 | NQ | NQ | NQ | NQ | NQ | NQ |
| Compound | 8 | 9 | 10 | 11 | 12 | 13 | 14 |
| oxodG | 7.2 | 3.0 | 2.9 | 3.5 | 2.1 | 9.3 | 3.9 |
| dG | NQ | NQ | NQ | NQ | NQ | 88 | NQ |

^aTitration experiments were performed by the method described in the footnote to Figure 1, and analyzed by the least-square method using a Kaleida Graph. Data of 1, 2, 8 and 9 were already reported in reference 10c.

Table 2. Equilibrium binding constants obtained by fluorescence quenching experiments in non-buffered CHCl₃ (K_s , 10⁵ M⁻¹)^a

| Compound | 1 | 2 | 3 | 4 | 5 | 6 | 7 |
|--|----------|----------|----------|----------|----------|----------|----------|
| oxodG | 36 | 71 | 160 | 130 | 130 | 320 | 130 |
| dG | 37 | 7.1 | 5.1 | 5.4 | 7.6 | 29 | 17 |
| $K_{\text{buffer}}/K_{\text{non-buffer}}$ | 0.20 | 0.31 | 0.19 | 0.22 | 0.12 | 0.1 | 0.43 |
| $K_{8\text{oxodG}}/K_{\text{dG}}^{\text{b}}$ | 1.0 | 10 | 31 | 24 | 17 | 11 | 7.6 |

| Compound | 8 | 9 | 10 | 11 | 12 | 13 | 14 |
|--|----------|----------|-----------|-----------|-----------|-----------|-----------|
| oxodG | 59 | 13 | 25 | 12 | 11 | 34 | 11 |
| dG | 28 | 40 | 39 | 15 | 11 | 820 | 6.6 |
| $K_{\text{buffer}}/K_{\text{non-buffer}}$ | 0.12 | 0.23 | 0.11 | 0.29 | 0.19 | 0.27 | 0.35 |
| $K_{8\text{oxodG}}/K_{\text{dG}}^{\text{b}}$ | 2.1 | 0.3 | 0.64 | 0.8 | 1.0 | 0.04 | 1.7 |

^aTitration experiments were performed by the method described in the footnote to Figure 1, except that TEA and AcOH were not added into the solution. ^bThe ratio of the binding constant (K_s) with 8-oxodG to dG in the non-buffered solution.

Fluorescence quenching experiments. A stock solution of the 3'-*O*-, 5'-*O*-diTBS protected 2'-deoxynucleoside (0-10 μM final concentration) was added to a solution of the 8-oxoGclamp analog (1 μM) in CHCl₃ containing 10 mM ETA and 2.7 mM AcOH at 25 °C. Fluorescence spectra were recorded with excitation at 365 nm. The fluorescence intensity at 450 nm was plotted against the concentration of the added 2'-deoxynucleoside analog and then analyzed by curve-fitting method based on 1:1 complexation as described previously.

Acknowledgements

This work was supported by a Grant-in-Aid for Scientific Research (S) from the Japan Society for the Promotion of Science (JSPS) and CREST from the Japan Science and Technology Agency. Z.L. is grateful for the Research Fellowship from Kobayashi International Scholarship Foundation.

References and notes

- 1 a) L. Risom, P. Moller, S. Loft, *Mutat. Res.* **2005**, 592, 119-137; b) A. M. Knaapen, N. G ng r, R. P. F. Schins¹, P. J. A. Borm, F. J. Van Schooten, *Mutagenesis* **2006**, 21, 225-236; c) A. Valavanidis, T. Vlahogianni, M. Dassenakis, M. Scoullas, *Ecotoxicol. Environ. Saf.* **2006**, 64, 178-189 ; d) B. Halliwell, *Biochem. J.* **2007**, 401, 1–11.
- 2 Examples, a) S. Shibutani, M. Takeshita, A. P. Grollaman, *Nature* **1991**, 349, 431-434; b) a recent report, G. E. Damsma¹, P. Cramer, *J. Biol. Chem.* **2009**, 284, 31658-31663; c) D. Bre geon, P.-A. Peignon, A. Sarasin, *PLoS Genet*, **2009**, 5, e1000577.
- 3 a) L. L. Wu, C.-C. Chiou, P.-Y. Chang, J. T. Wu, *Clin. Chim. Acta*, **2004**, 339, 1-9; b) H. Kasai, *Mutat. Res.* **1997** 387, 147–163; c) K. P. Cantor, *Toxicology* **2006**, 221, 197-204; d) A. R. Collins, *Am. J. Clin. Nutr.* **2005**, 81, 261S-267S.
- 4 Examples, a) P. Jenner, C. W. Olanow, *Neurology* **1996**, 47, S161-170; b) S. Loft, H. E. Poulsen, *J. Mol. Med.* **1996**, 74, 297-312; c) I. Dalle-Donne, R. Rossi , R. Colombo, D. Giustarini, A. Milzani, *Clinical Chem.* **2006**, 52, 601-623; d) Y. Nakabeppu, D. Tsuchimoto, H. Yamaguchi, K. Sakumi; *J. Neurosci. Res.* **2007**, 85, 919-934, e) T. T. Saxowsky, K. L. Meadowsa, A. Klungland, P. W. Doetsch, *Proc. Nat. Acad. Sci.* **2008**, 105 18877-18882.
- 5 a) V. A. Bohr, *Free Radic. Biol. Med.* **2002**, 32, 804-812; b) G. Barja, *Trends Neurosci.* **2004**, 27, 595-600; c) M. F. Beal, *Ann. Neurol.* **2005**, 58, 495–505; d) S. Moriwaki, Y. Takahashi, *J. Dermatol. Sci.* **2008**, 50, 169-176.
- 6 a) J. P. Pouget, T. Douki, M. J. Richard J. Cadet, *Chem. Res. Toxicol.* **2000**, 13, 541-549; b) A. Siomek, A. Rytarowska, A. Szaflarska-Poplawska, D. Gackowski, R. Rozalski, T. Dziaman, M. Czerwionka-Szaflarska, R. Olinski, *Carcinogenesis* **2006**, 27, 405-408; c) T. Hofer, A. Y. Seo, M. Prudencio, C. Leeuwenburgh, *Biol. Chem.* **2006**, 387, 103-113.
- 7 a) H. Wiseman, H. Kaur, B. Halliwell, *Cancer Lett.* **1995**, 93, 113-120; b) M. Dizdaroglu, P. Jaruga, M. Birincioglu, H. Rodriguez, *Free Radic. Biol. Med.* **2002**, 32, 1102-1115; c) M. Lodovici, C. Casalini, R. Cariaggi, L. Michelucci, P. Dolara, *Free Radic. Biol. Med.* **2000**, 28, 13-17; d) Y. Nakabeppu, D. Tsuchimoto, M. Furuichi, K. Sakumi, *Free Radic. Res.* **2004**, 38, 423-429; e) Y. Nakae, P. J. Stoward, I. A. Besselov, R. J. Melamede, S. S. Wallace, *Histochem. Cell Biol.* **2005**, 124,

335-345.

- 8 a) M. L. Gielazyn, A. H. Ringwood, W. W. Piegorsch, S. E. Stancyk, *Mut. Res.* **2003**, *542*, 15-22; b) A. Mugweru, B. Wang, J. Rusling, *Anal. Chem.* **2004**, *76*, 5557-5563; c) L. Dennany, R. J. Forster, B. White, M. Smyth, J. F. Rusling, *J. Am. Chem. Soc.* **2004**, *126*, 8835-8841; d) H. Orimo, N. Mei, S. Boiteux, Y. Tokura, H. Kasai, *J. Radiat. Res.* **2004**, *45*, 455-460.
- 9 a) R. P. Soultanakis, R. J. Melamede, I. A. Bernalob, S. S. Wallace, K. B. Beckman, B. N. Ames, D. J. Taatjes, W. M. W. Janssen-Heininger, *Free Radic. Biol. Med.* **2000**, *28*, 987-998; b) C. C. Chiou, P. Y. Chang, E. C. Chan, T. L. Wu, K. C. Tsao, J. T. Wu, *Clin. Chim. Acta* **2003**, *334*, 87-94; c) N. Machella, F. Regoli, A. Cambria, R. M. Santella, *Mar. Environ. Res.* **2004**, *58*, 725-729; d) Y. Nakae, P. J. Stoward, I. A. Bernalob, R. J. Melamede, S. S. Wallace, *Histochem. Cell Biol.* **2005**, *124*, 335-345.
- 10 a) O. Nakagawa, S. Ono, Z. Li, A. Tsujimoto, S. Sasaki, *Nucleic Acids Symp. Ser.*, **2006**, *50*, 21-22; b) O. Nakagawa, S. Ono, Z. Li, A. Tsujimoto, S. Sasaki, *Nucleosides Nucleotides Nucleic Acids*, **2007**, *26*, 645-649, c) O. Nakagawa, S. Ono, Z. Li, A. Tsujimoto, S. Sasaki, *Angew. Chem. Int. Ed.* **2007**, *46*, 4500-4503; d) T. Nasr, Z. Li, O. Nakagawa, Y. Taniguchi, S. Ono, S. Sasaki, *Bioorg. Med. Chem. Lett.*, **2009**, *19*, 727-730.
- 11 (a) S. Tsuzuki, K. Honda, T. Uchimaru and M. Mikamia, *J. Chem. Phys.*, **2004**, *120*, 647-659. (b) R. Podeszwa and K. Szalewicz, *Phys. Chem. Chem. Phys.*, **2008**, *10*, 2735- 2746.
- 12 M. Torimura, S. Kurata, K. Yamada, T. Yokomaku, Y. Kamagata, T. Kanagawa, R. Kurane, *Anal. Sci.* **2001**, *17*, 155-160.
- 13 M. S. Cubberley and B. L. Iverson, *J. Am. Chem. Soc.* **2001**, *123*, 7560-7563